



Reduction of Light Rare Earths and a Proposed Process for Nd Electrorecovery Based on Ionic Liquids

E. Bourbos¹ · I. Giannopoulou¹ · A. Karantonis² · I. Paspaliaris¹ · D. Panias¹

Published online: 2 August 2018

© The Minerals, Metals & Materials Society 2018

Abstract

Electrodeposition of the rare-earth metals La, Sm, Nd, and Dy from solution in the ionic liquids *N*-butyl-*N*-methylpyrrolidinium bistriflimide (BMPTFSI) and trimethyl butylammonium bistriflimide (Me₃NBuTFSI) was studied in this work. Both ionic liquids are hydrophobic and present a wide electrochemical window as well as satisfactory ionic conductivity, rendering them promising electrolytes for electroreduction of rare-earth elements. Cyclic voltammetry (CV) performed using a Pt electrode in a three-electrode cell revealed that the rare-earth cations could indeed be reduced to the metallic state in the above-mentioned ionic liquids. Furthermore, electrodeposition of the rare earths was realized on copper substrate under potentiostatic conditions of -3.1 V versus Ag/0.1 M AgNO₃ in acetonitrile at 25 °C for 5 h. Analysis of the electrodeposits by scanning electron microscopy (SEM) and energy-dispersive X-ray spectroscopy (EDS) revealed that electrodeposition of the rare earths was feasible using these ionic liquids as the electrolytic medium. Finally, with the aim of identifying a sustainable metallurgical process for electrorecovery of rare earths, a two-compartment electrolytic cell was developed and tested for production of neodymium from a Nd(TFSI)₃/BMPTFSI electrolyte.

Keywords Electrodeposition · Ionic liquids · Pyrrolidinium · Rare earths · Neodymium

Introduction

Production of rare-earth metals and alloys is conventionally performed by electrolysis of high-temperature molten salts, which involves a highly corrosive environment and high energy demands. An alternative is use of the electrochemical route, using ionic materials with low melting temperature [1]. Since the middle of the 20th century, a significant amount of work has been carried out with the aim of developing such molten salts with lower melting temperature. The major goal of such work was synthesis of a lower-temperature melt for deposition of aluminum,

which led to the development of Li⁺/K⁺/AlCl₃ eutectics with melting point close to 100 °C [2, 3]. The introduction of quaternary ammonium, pyrrolidinium, and imidazolium salts has pushed the melting point down to ambient conditions [4]. The term “ionic liquids” was coined to distinguish these lower-temperature ionic liquids from their high-temperature analogs predominantly composed of inorganic ions [1, 4]. Several applications of ionic liquids have been tested, being as diverse as fuel desulfurization and precious metal processing, but few have yet to come to practical fruition. Several other processes are also at pilot plant scale, and some ionic liquids are used commercially as additives, e.g., as binders in paints [4]. At this point, it must be pointed out that, while deposition of a wide range of metals from numerous ionic liquids has been demonstrated, practical aspects of controlling the morphology of such deposits have not been significantly addressed due to the complex nature of the process parameters that still need to be elucidated [4, 5]. Despite the difficulty in describing mass transport and material growth in ionic liquids, ionic liquids offer tempting advantages in comparison with aqueous baths, which makes understanding their properties vitally important.

The contributing editor for this article was U. Pal.

✉ E. Bourbos
ebourbos@metal.ntua.gr

¹ School of Mining and Metallurgical Engineering, National Technical University of Athens, 9 Iroon Polytechniou, 15780 Zografou, Athens, Greece

² School of Chemical Engineering, National Technical University of Athens, 9 Iroon Polytechniou, 15780 Zografou, Athens, Greece

Concerning the use of ionic liquids in nonferrous metallurgy [6], it must be pointed out that, even though deposition of a wide range of nonferrous metals from numerous ionic liquids has been studied and demonstrated [7], the complex nature of the associated process parameters limits industrial applications. An important disadvantage of room-temperature ionic liquids (RTILs) is their low electrical conductivity, which is about 10 times lower than that of molten electrolytes currently applied for production of nonferrous metals [7, 8]. However, the possibility of using ionic liquids at temperatures above 100 °C, where their electrical conductivity is substantially increased, enhances their prospects for application as electrolytes [1, 4]. The ongoing development of ionic liquids may lead to materials that exhibit even better conduction; preliminary studies have proven that RTILs are effective solvents and electrolytes for reactive metals such as Li, Nb, Ta, and Mg [9–11] as well as Al and Ce [12–16].

Glukhov et al. [17] reported reduction of Y, Gd, and Yb in the ionic liquid BMPCF₃SO₃ on both platinum and copper electrodes. Voltammetric curves obtained using Pt electrodes in the systems of Y and Gd with this IL revealed a cathodic peak with maximum value of -2.6 V (rel. Ag/0.1 M Cl⁻), which was attributed to reduction of the trivalent cation to the metallic state. Electrodeposition of these metals was performed under potentiostatic or galvanostatic conditions, forming a tenuous black precipitate on the surface of the electrode. It was also shown that reduction of Yb(III) to the metallic form occurs stepwise via Yb(II) formation, and that the limiting stage of the cathodic process is the adsorption of the metal cation onto the electrode. Legeai et al. [18] showed that reduction of La in OMPTFSI is an irreversible reaction and that electrodeposition of La from this ionic liquid under potentiostatic polarization conditions of -1.5 V (versus Ag/AgCl) at 298 K for 120 min resulted in a cathodic deposit with a thick La film of 350 nm.

In addition, Yamagata et al. [19] used cyclic voltammetry to study the redox reactions of the Sm(III)/Sm(II) couple in the ionic liquid BMPTFSI using a glassy-carbon electrode and determined the redox reactions to be quasireversible or irreversible. They also studied the electrochemistry of Yb(III) in BMPTFSI using cyclic voltammetry, observing a cathodic and an anodic peak at around -0.95 V (versus Ag/Ag⁺), which they attributed to reduction of Yb(III) and oxidation of Yb(II), respectively. The electrochemical behavior of Eu(III) in BMPTFSI was researched by Rao et al. [20] using glassy-carbon and stainless-steel electrodes, at various temperatures. The cyclic voltammograms revealed a quasireversible behavior of the Eu(III)/Eu(II) redox couple and an irreversible behavior of the Eu(II)/Eu(0) couple, which presented a cathodic peak that was attributed to reduction of Eu(II) to

its metallic state. In the same ionic liquid (BMPTFSI) but containing chloride anions, Hussey et al. [21] studied the electrochemical and spectroscopic behavior of Nd(III) and Pr(III). According to their results, electrolytic dissolution of both metals in this ionic liquid system produced only the respective trivalent cations, which could be reduced to the Ln(II) state, but the resulting divalent species exhibited only transient stability, undergoing rapid disproportionation to Ln(III) and Ln(0) states.

Glukhov et al. [17] investigated reduction of Y, Gd, and Yb in the ionic liquid Bu₃MeNCF₃SO₃ and concluded that deposition of these metals is only possible on a copper substrate but does not occur on platinum. Bhatt et al. [22] reported reduction of selected lanthanide cations (La, Sm, and Eu) to the zero-valent state in the ionic liquid Me₃NBuTFSI. The lanthanide cations were introduced into the ionic liquid as TFSI hydrate complexes. Cyclic voltammograms revealed a cathodic peak at -2.4 V versus Fc⁺/Fc for the lanthanum system, which was attributed to reduction to the metallic state, whereas two peaks were observed for the Sm and Eu systems; the less negative one was associated with the (III)/(II) reaction, and the more negative one with the reduction to the metallic state.

The scope of the work presented herein is study of electrodeposition of rare earths from ionic liquids and to design a potential process for electrorecovery of metallic neodymium at ambient temperature using such ILs. Taking into account literature data and preliminary screening experiments, electrodeposition of rare earths was researched in two ionic liquids, viz. BMPTFSI and Me₃NBuTFSI. These hydrophobic ionic liquids present good properties for electrodeposition of light rare-earth elements, namely wide electrochemical stability, low hygroscopicity, low viscosity, and significant ionic conductivity. The electrochemical stability of the mentioned ionic liquids and the reduction of rare-earth cations in the ionic liquids BMPTFSI and Me₃NBuTFSI as the electrolytic medium were tested using cyclic voltammetry. Moreover, chronoamperometry was performed in the same systems for electrodeposition of rare-earth metals, and the deposits were examined by scanning electron microscopy and evaluated by EDS analysis. Furthermore, a promising process for neodymium electrorecovery was developed based on cyclic voltammetry and chronoamperometry tests, and the final electrodeposits were evaluated by X-ray photoelectron spectroscopy (XPS) and SEM-EDS analyses.

Materials and Methods

The ionic liquid BMPTFSI was supplied by Iolitec, and Me₃NBuTFSI by Solvionic. The moisture content was 73 ppm for BMPTFSI and less than 100 ppm for

$\text{Me}_3\text{NBuTFSI}$, according to data provided by each company, and they were used as received. Lanthanum nitrate hexahydrate, neodymium nitrate hydrate, and samarium trifluoromethanesulfonate were purchased from Alfa Aesar. Dysprosium bistriflimide trihydrate was synthesized by reaction of dysprosium oxide purchased from Alfa Aesar and trifluoromethanesulfonimide from Sigma Aldrich [20]. The nitrate salts and bistriflimide salt were heated at 100 °C under vacuum for 72 h and dissolved in pure acetone, to which the proper amount of electrolyte was subsequently added to achieve solution concentration on the order of 0.06 M. The solution was placed at 60 °C under vacuum for approximately 2 h to remove acetone, then at 100 °C under vacuum for 24 h to remove residual water. Cyclic voltammetry tests were performed in a three-mili-electrode cell (PAR) connected to a VersaSTAT 3 potentiostat (PAR); the obtained experimental data were analyzed using VersaStudio software (PAR). The working electrode was a platinum disk of $d = 1.98$ mm, with a Pt wire immersed directly into the solution as a counterelectrode, and finally the redox couple $\text{Ag}/0.1$ M AgNO_3 in acetonitrile as reference electrode, while for the 24-h chronoamperometry measurements, a Pt wire calibrated versus the reversible Fc/Fc^+ couple was employed as a pseudoreference electrode due to the evaporation of acetonitrile. The ferrocene/ferrocenium (Fc/Fc^+) redox potential was recorded versus the Pt pseudoreference electrode after direct dissolution of 10 mM ferrocene in both ionic liquids under study and was used as the reference potential. The working electrode was polished using 1- μm alumina paste on a velvet pad and electrochemically in 1 M sulfuric acid. Although BMPTFSI exhibits hydrophobic characteristics and is stable under normal atmospheric conditions, the cyclic voltammetry and chronoamperometry measurements were performed under inert conditions, to minimize oxygen and moisture contamination, in an Ar atmosphere inside a Pure Lab glove box supplied by INERT, where oxygen and moisture were kept below 20 and 50 ppm, respectively. The morphology of the electrodeposits was examined using a scanning electron microscope (JEOL6380LV) equipped with an energy-dispersive spectrometer. Where needed, chemical analysis to measure the neodymium concentration in the prepared solutions was performed using a PerkinElmer 2100 atomic absorption spectrophotometer.

The photoemission experiments were carried out in an ultrahigh-vacuum (UHV) system consisting of a fast entry specimen assembly, a sample preparation chamber, and an analysis chamber. The base pressure in both chambers was 1×10^{-9} mbar. The unmonochromatized Mg K_{α} line at 1253.6 eV and an analyzer pass energy of 97 eV, giving a full-width at half-maximum (FWHM) of 1.7 eV for the Au $4f_{7/2}$ peak, were used in all XPS measurements. The

XPS core-level spectra were analyzed using a fitting routine that can decompose each spectrum into individual mixed Gaussian–Lorentzian peaks after Shirley background subtraction. The samples were analyzed in vials in an inert atmosphere and inserted into the UHV system through a glove bag in He atmosphere to prevent further surface oxidation.

Survey scans were recorded for all samples, while Nd 3d, S 2p, F 1s, O 1s, and C 1s core-level peaks were recorded in detail.

Results

Cyclic Voltammetry of Rare-Earth Solutions in Ionic Liquids

The electrochemical window of BMPTFSI was determined at room temperature by cyclic voltammetry (Fig. 1); the cathodic limit of the electrolyte was found to be at -3.4 V versus Ag/Ag^+ , assuming a threshold of 1 mA/cm^2 [2]. Figure 1 shows the cyclic voltammogram recorded in the BMPTFSI/ $\text{La}(\text{NO}_3)_3$ system. Generation of an intense cathodic peak begins at -2.2 V versus Ag/Ag^+ , attributed to the reduction of the trivalent lanthanum cation (La^{3+}) to the metallic state. The absence of a corresponding anodic peak in the reverse scan allows the assumption that the lanthanum reduction is irreversible [15, 16]. Moreover, the cathodic peak at -1 V can be ascribed to the reduction of hydrogen cations, due to small amounts of water [1] that are inevitably present, while the narrow shoulder at -1.5 V can be attributed either to an adsorption reaction of La^{3+} onto the electrode prior to the reduction of lanthanum [15], or to an underpotential deposition phenomenon taking place over this range of potential.

Typical cyclic voltammograms of the BMPTFSI/ $\text{Nd}(\text{NO}_3)_3$, BMPTFSI/ $\text{Dy}(\text{TFSI})_3$, and BMPTFSI/ $\text{Sm}(\text{OTf})_3$ systems are presented in Figs. 2, 3, and 4,

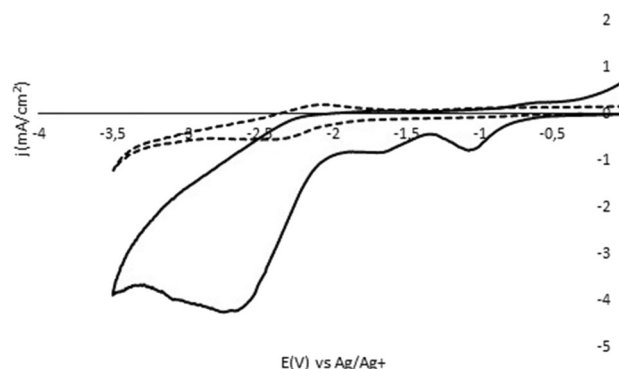


Fig. 1 CVs recorded at scan rate of 20 mV/s and 25 °C for BMPTFSI (dashed line) and 0.06 M $\text{La}(\text{NO}_3)_3$ in BMPTFSI (solid line)

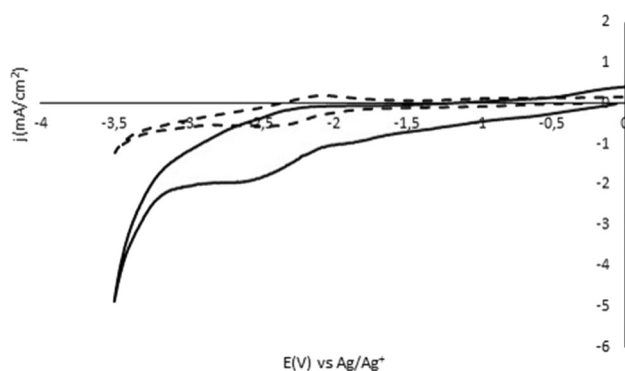


Fig. 2 CVs recorded at scan rate of 20 mV/s and 25 °C for BMPTFSI (dashed line) and 0.06 M $\text{Nd}(\text{NO}_3)_3$ in BMPTFSI (solid line)

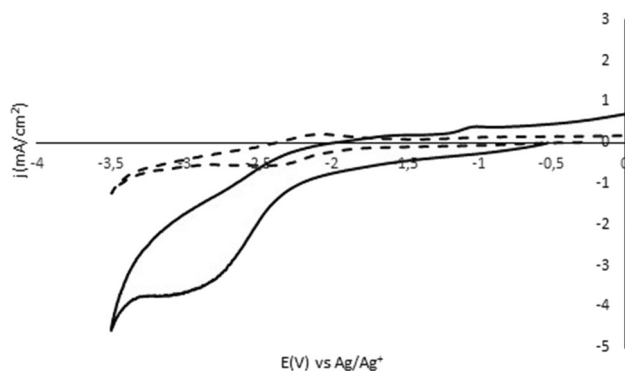


Fig. 3 CVs recorded at scan rate of 20 mV/s and 25 °C for BMPTFSI (dashed line) and 0.06 M $\text{Dy}(\text{TFSI})_3$ in BMPTFSI (solid line)

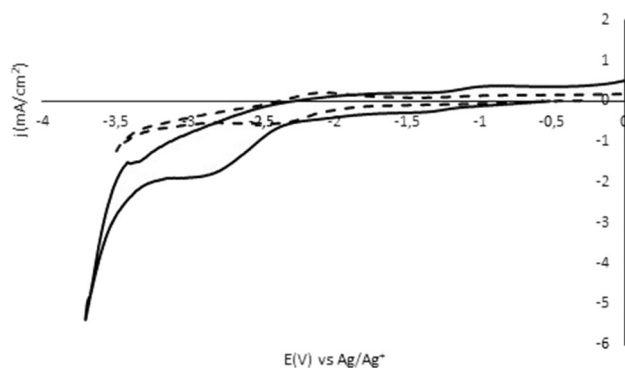


Fig. 4 CVs recorded at scan rate of 20 mV/s and 25 °C for BMPTFSI (dashed line) and 0.06 M $\text{Sm}(\text{OTf})_3$ in BMPTFSI (solid line)

respectively. In the BMPTFSI/ $\text{Nd}(\text{NO}_3)_3$ system (Fig. 2), a cathodic plateau starts to form at potential values more cathodic than -2.2 V versus Ag/Ag^+ , associated with the corresponding reduction of trivalent Nd cations to the metallic state, while no peaks related to presence of water are observed. Moreover, a slight shoulder is also observed in Fig. 2, suggesting an Nd^{3+} adsorption reaction onto the electrode, prior to the reduction of neodymium [15], or to

an underpotential deposition phenomenon taking place over this range of potential, similarly to the lanthanum system reported above. Figure 3 shows the cyclic voltammogram recorded for the BMPTFSI/ $\text{Dy}(\text{TFSI})_3$ system. A cathodic current begins after -2.3 V versus Ag/Ag^+ , forming a cathodic loop, which indicates the reduction of Dy^{3+} to the zero-valent state. On scanning the potential to values more cathodic than -3.4 V versus Ag/Ag^+ , a second cathodic current, related to the decomposition reaction of the ionic liquid, appears. Finally, Fig. 4 presents the cyclic voltammogram for the BMPTFSI/ $\text{Sm}(\text{OTf})_3$ system. A cathodic peak starts to form when the potential is scanned to values more cathodic than -2.3 V versus Ag/Ag^+ , suggesting that reduction of metallic Sm occurs. No anodic currents are detected in Figs. 1, 2, 3, and 4, implying that the reduction of the cations under study in this ionic liquid is irreversible.

In addition, the electrochemical window of $\text{Me}_3\text{NBuTFSI}$ was determined at room temperature by cyclic voltammetry (Fig. 5); its cathodic limit was found to be -3.6 V versus Ag/Ag^+ . The cyclic voltammogram recorded in the $\text{Me}_3\text{NBuTFSI}/\text{La}(\text{NO}_3)_3$ system (Fig. 5) reveals a cathodic plateau that begins to form at -2.2 V versus Ag/Ag^+ , which can be attributed to the reduction of trivalent lanthanum cation (La^{3+}) to the zero-valent state. Contrary to what was presented in Fig. 1 for the BMPTFSI/ $\text{La}(\text{NO}_3)_3$ system, the cyclic voltammogram recorded for the $\text{Me}_3\text{NBuTFSI}/\text{La}(\text{NO}_3)_3$ system does not present a cathodic peak, but rather a broad cathodic plateau, while there are no signs of a cathodic loop at -1.5 V that could indicate an adsorption phenomenon or underpotential deposition. The cyclic voltammogram of the $\text{Me}_3\text{NBuTFSI}/\text{Nd}(\text{NO}_3)_3$ system is presented in Fig. 6, showing the generation of a cathodic current at -2.5 V versus Ag/Ag^+ , which indicates the reduction of the trivalent Nd cation to metallic Nd. The reduction potential of Nd cations in this system is shifted to slightly more cathodic values in

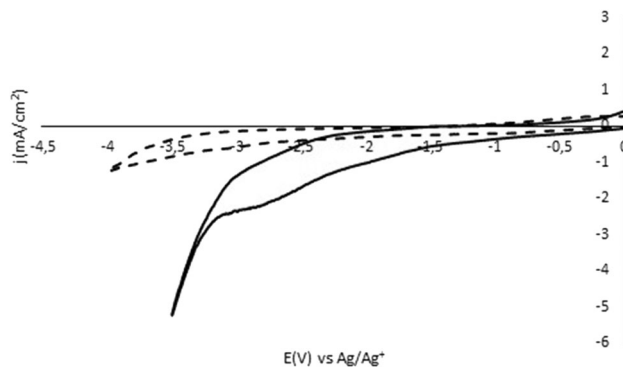


Fig. 5 CVs recorded at scan rate of 20 mV/s and 25 °C for $\text{Me}_3\text{NBuTFSI}$ (dashed line) and 0.06 M $\text{La}(\text{NO}_3)_3$ in $\text{Me}_3\text{NBuTFSI}$ (solid line)

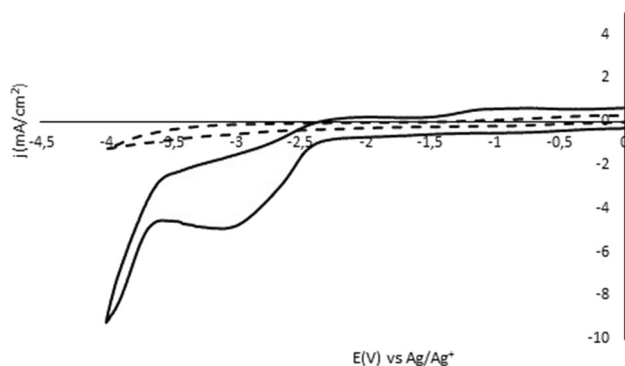


Fig. 6 CVs recorded at scan rate of 20 mV/s and 25 °C for Me₃NBUtFSI (dashed line) and 0.06 M Nd(NO₃)₃ in Me₃NBUtFSI (solid line)

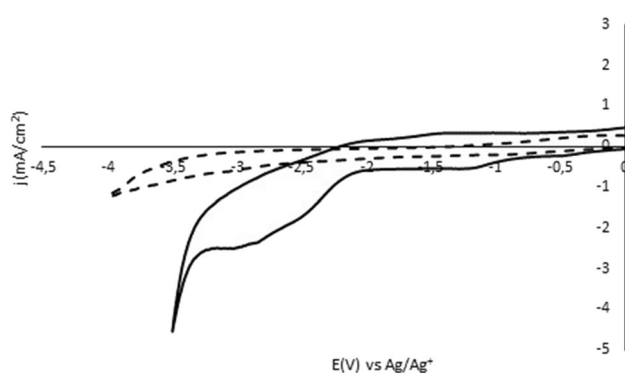


Fig. 7 CVs recorded at scan rate of 20 mV/s and 25 °C for Me₃NBUtFSI (dashed line) and 0.06 M Sm(OTf)₃ in Me₃NBUtFSI (solid line)

comparison with the BMPTFSI/Nd(NO₃)₃ system presented in Fig. 2. Finally, Fig. 7 shows the cyclic voltammogram recorded for the Me₃NBUtFSI/SmOTf₃ system; the reduction of Sm cations is confirmed by the cathodic peak that forms when scanning the potential to values more cathodic than −2.3 V versus Ag/Ag⁺. The absence of a corresponding anodic peak in the reverse scan in Figs. 5, 6, and 7 allows the assumption that the reduction of the studied cations is irreversible in the Me₃NBUtFSI ionic liquid, similar to the finding for the BMPTFSI ionic liquid presented above. This may suggest that the bistriflimide anion that is common to these two ionic liquids is mainly responsible for hindering the oxidation of the electrodeposited metal [18].

Electrodeposition of Rare Earths from Ionic Liquids

Electrodeposition of the above-studied rare-earth metals was attempted under potentiostatic conditions of −3.1 V and 25 °C on a copper substrate in BMPTFSI and Me₃NBUtFSI for 5 h [21, 22]. The morphology, structure, and

shape of the resulting electrodeposits were examined by scanning electron microscopy with energy-dispersive spectrometry analysis, which revealed the presence of the rare earths, thus indicating their reduction. The La, Nd, Dy, and Sm electrodeposits along with the EDS analysis in BMPTFSI are presented in Figs. 8 and 9, respectively. The lanthanum electrodeposit (Fig. 8a) was dispersed and granular, forming aggregates. The elevated concentrations of sulfur and fluorine indicate that the electrolyte was not totally removed from the surface of the electrode, a finding that is common to all the presented electrodeposits and that can be attributed to the high viscosity of the ionic liquid solutions at ambient temperature. The electrolyte is hydrophobic, so it could not be removed from the electrode by simple rinsing with water. In order to remove it, the electrode should be rinsed with acetone or another polar organic solvent, but this leads to immediate oxidation of the electrodeposited metal accompanied by elevated oxygen concentrations in EDS analysis and the formation of a white layer on top of the electrode. The Sm deposit (Fig. 8d) resembles that of La but is more massive with the formation of flakes. The Nd deposit was more compact and concrete (Fig. 8b) compared with all the other deposits. Finally, the Dy deposit was microgranular with distinct particles in the range of 1–5 μm (Fig. 8c).

The EDS spectra revealed successful electrodeposition of the rare earths, while the presence of copper is due to detection of the substrate used (Fig. 9). In all cases, the presence of impurities attributed to the ionic liquid used was also evident.

The electrodeposits of La, Nd, and Sm along with results of EDS analysis in Me₃NBUtFSI are presented in Figs. 10 and 11, respectively. Figure 10a presents the electrodeposit of lanthanum, where the existence of small nuclei is noticeable. The electrodeposition began at these small nuclei, forming larger clusters that were identified as lanthanum crystals by EDS analysis. The electrodeposits were mainly observed at the edges of the electrode. Figure 10b and c present the electrodeposited neodymium and samarium, respectively. Sulfur and fluorine were also detected by EDS analysis, as in the case of the BMPTFSI ionic liquid.

The EDS spectra confirming the electrodeposition of the rare earths tested are presented in Fig. 11.

Metallurgical Process for Production of Rare Earths Based on Electrolysis in Ionic Liquids

The results presented above establish that La, Nd, Sm, and Dy can indeed be electrodeposited from these ionic liquids, even at room temperature. Nevertheless, one crucial feature of such electrolysis processes is yet to be addressed, viz. the reactions taking place at the anode. In the systems under consideration, the rare-earth salts were nitrates,

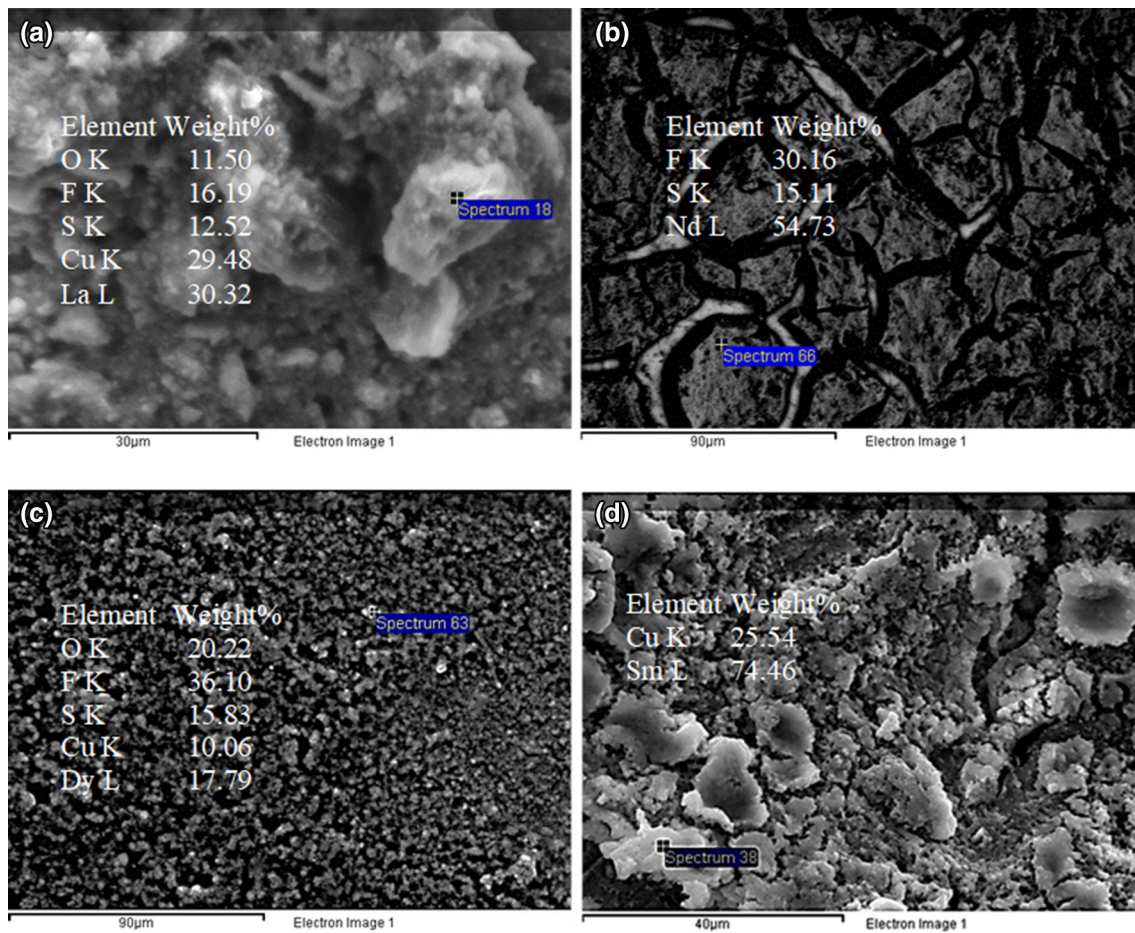


Fig. 8 SEM images of electrodeposited **a** lanthanum, **b** neodymium, **c** dysprosium, and **d** samarium (color figure online)

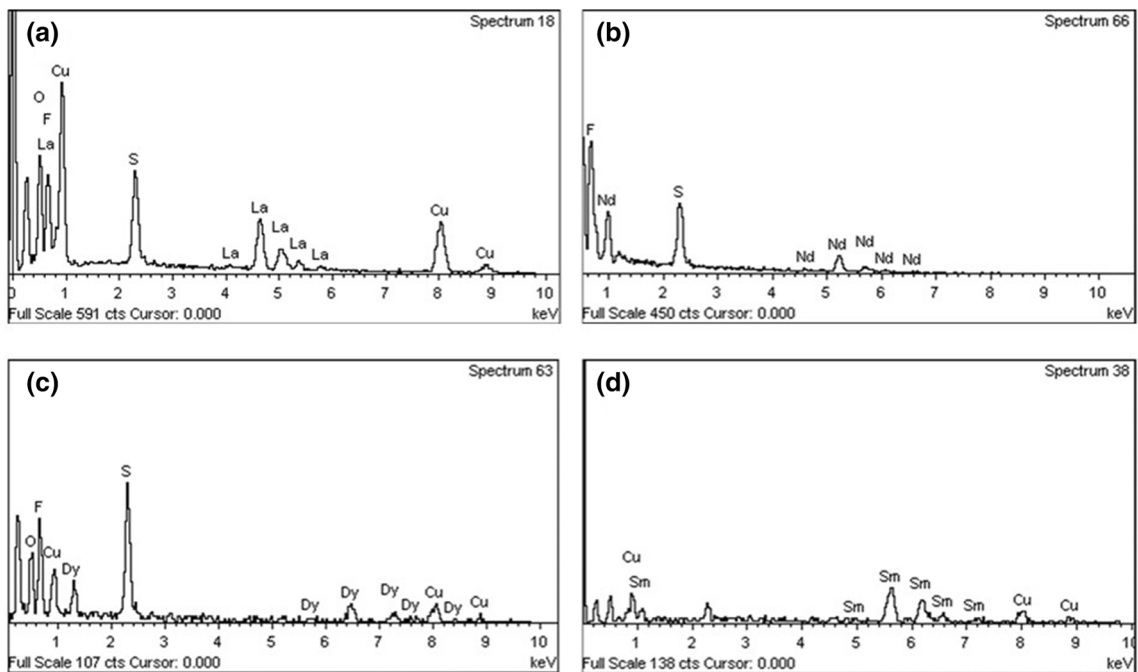


Fig. 9 EDS spectra of electrodeposited **a** lanthanum, **b** neodymium, **c** dysprosium, and **d** samarium

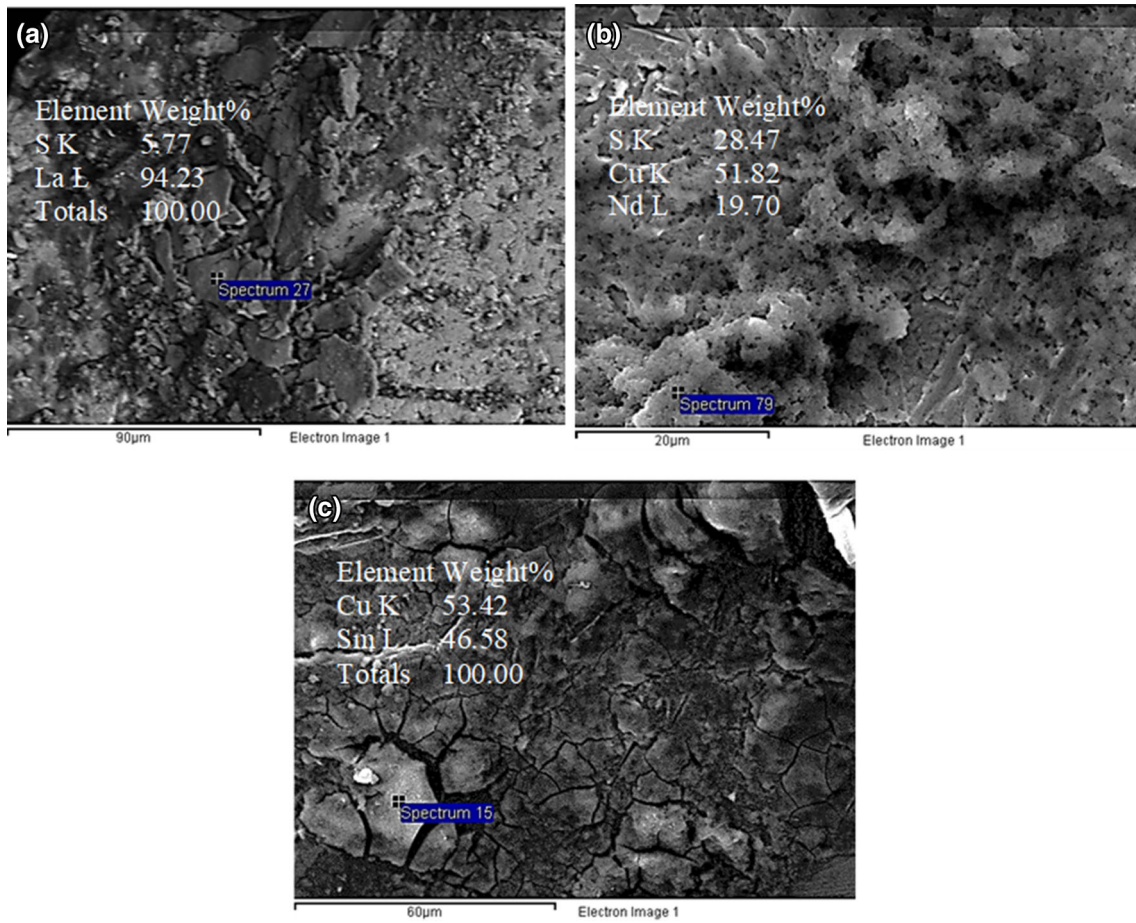


Fig. 10 SEM images of electrodeposited **a** lanthanum, **b** neodymium, and **c** samarium (color figure online)

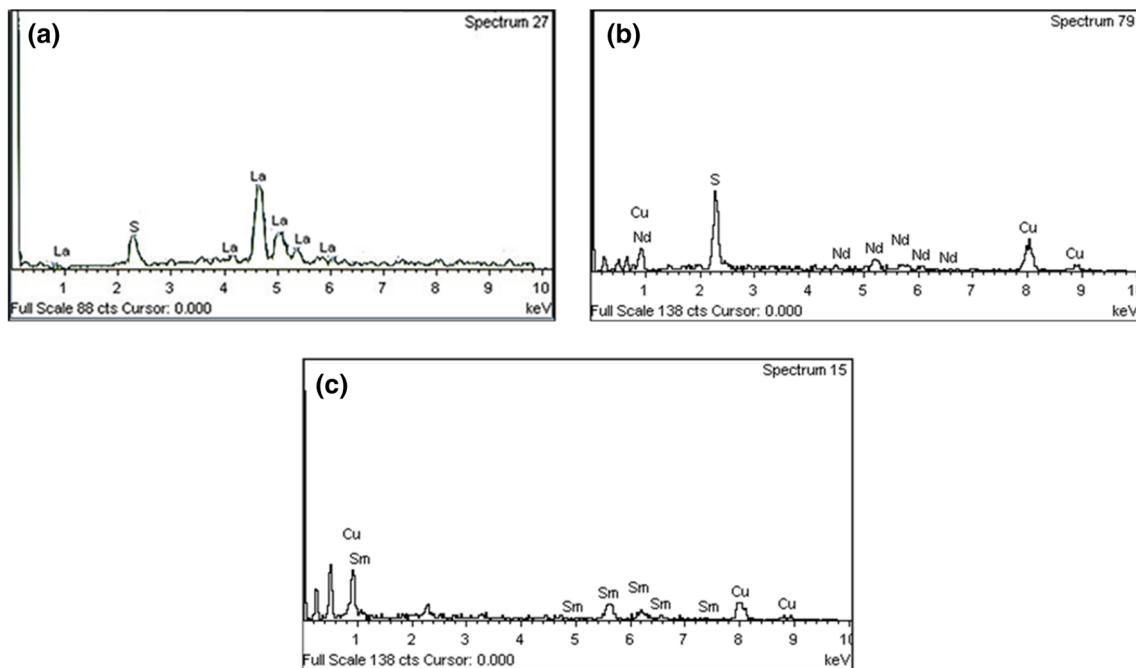


Fig. 11 EDS spectra of electrodeposited **a** lanthanum, **b** neodymium, and **c** samarium (color figure online)

trifluoromethanesulfonates, and bistriflimides. Among these, bistriflimides can be easily dissolved in BMPTFSI [23] and are oxidized on the anode at a potential of +2.4 V versus Ag/0.1 M AgNO₃ in acetonitrile at 25 °C, as seen in Fig. 12.

Nevertheless, bistriflimide salts have a very high cost and are difficult to synthesize, making them inapplicable as sacrificial metal carrier salts. Triflate (trifluoromethanesulfonate) salts, which can also be anodically oxidized, are less expensive than bistriflimide salts, but are still high cost, also making their use economically inefficient. Finally, nitrate salts have the lowest cost and can also be dissolved in BMPTFSI, making them of remarkable interest from a metallurgical point of view. However, they are in the highest oxidative state and thus cannot be oxidized further on the anode surface. This means that, in systems where the rare earths are dissolved in the form of nitrate salts, the electrolyte (BMPTFSI) is gradually decomposed due to anodic oxidation of the TFSI[−] anions of the ionic liquid, making such processes unattractive from the metallurgical and economic points of view. To overcome the problem of the anodic reaction, it was attempted to dissolve relatively cheap neodymium chloride and fluoride salts in the ionic liquid BMPTFSI directly under stirring at 130 °C for 24 h, to provide easily oxidized anionic species in the electrolyte (F[−] and Cl[−] anions are oxidized at +2.1 and 0.6 V versus Ag/0.1 M AgNO₃ in acetonitrile at 25 °C, respectively) and thus avoid the anodic decomposition of the ionic liquid. Unfortunately, it was found that both Nd fluoride and chloride salts dissolved only sparingly in the BMPTFSI ionic liquid.

Taking into account that (a) BMPTFSI is a good electrolyte but not a good solvent for rare-earth metal salts except those that share a common anion with the ionic liquid [namely REE(TFSI)₃ salts] and (b) direct electrolysis in the BMPTFSI/REE(TFSI)₃ system is not attractive from an economic point of view, the idea of Nd

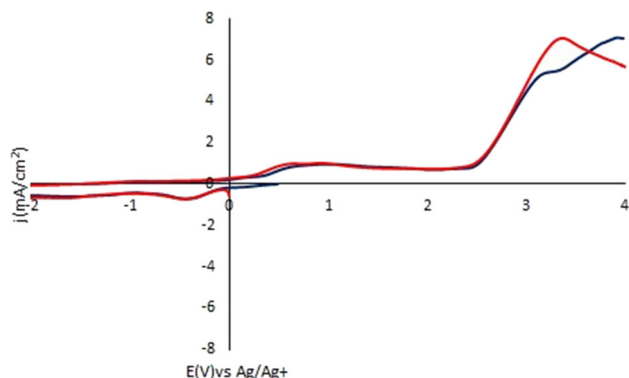


Fig. 12 Anodic oxidation of TFSI[−] anions in BMPTFSI (red curve) and Me₃NBuTFSI (blue curve) (color figure online)

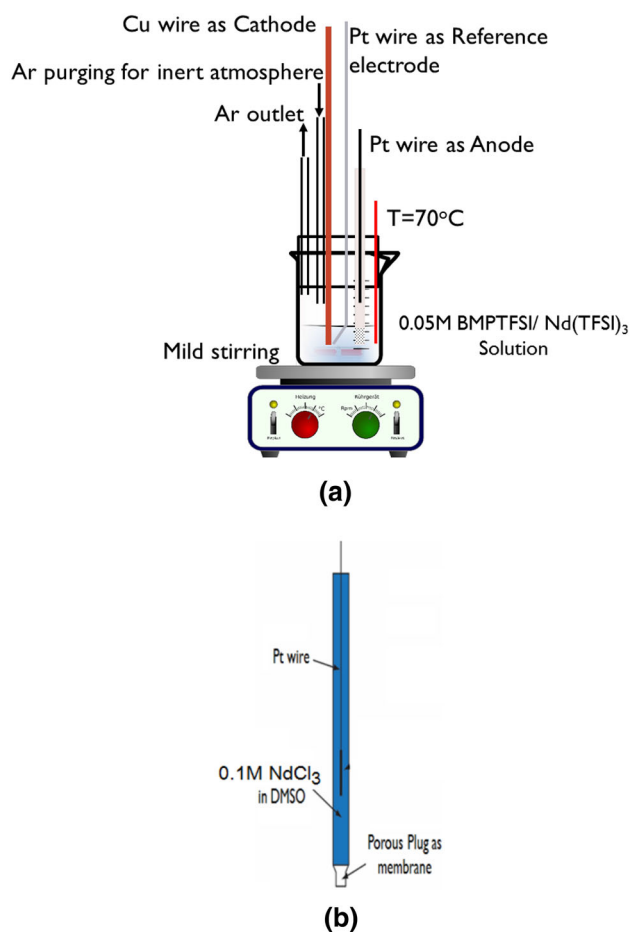


Fig. 13 **a** Two-compartment electrolytic cell setup and **b** detail of anolyte compartment (color figure online)

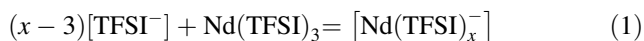
electrolysis in a two-compartment cell was developed, as shown in Fig. 13.

This preliminary, very small-scale two-compartment electrolytic cell setup consisted of (a) a cathodic compartment containing a copper wire as a cathode immersed in 0.05 M Nd(TFSI)₃/BMPTFSI solution, (b) an anodic compartment containing a Pt wire immersed in 0.1 M NdCl₃/dimethylsulfoxide (DMSO) solution, separated from the cathodic compartment through a porous plug that plays the role of a semipermeable ceramic membrane, and (c) a Pt wire as a pseudoreference, calibrated versus a reversible Fc/Fc⁺ couple electrode, located very close to the surface of the Cu cathode. The cell consisted of a glass beaker, tightly closed by a cork to keep the position of the electrodes steady. Finally, the cell was thermostated and stirred gently using a magnetic stirrer. The following phenomena take place during cell operation:

Cathodic Compartment

During the dissolution of Nd(TFSI)₃ in the BMPTFSI, the TFSI[−] anions of the ionic liquid solvate the Nd cations,

forming negatively charged neodymium complexes $\text{Nd}(\text{TFSI})_4^-$ [24, 25] or $\text{Nd}(\text{TFSI})_5^-$ [26] according to the following reaction:



Therefore, the catholyte consists of BMP^+ cations and TFSI^- anions as well as solvated neodymium anions $\text{Nd}(\text{TFSI})_4^-$ in very large ionic associations, making the solution more viscous than the initial BMPTFSI ionic liquid. On polarizing the cathode at a potential lower than -2.2 V, the BMP^+ cations electromigrate towards the cathode, carrying TFSI^- and $\text{Nd}(\text{TFSI})_4^-$ anions due to the very strong ionic association in ionic liquids, and forming a thick boundary layer on the cathode surface. The anionic speciation of neodymium hinders its electromigration towards the cathode, and the concentration of $\text{Nd}(\text{TFSI})_4^-$ anions inside the cathode surface boundary layer is more or less dependent on the very strong ionic association in the ionic liquid solutions. At the electrode interface, the TFSI^- anionic ligands are dissociated from the Nd^{3+} centers, making electroreduction according to the following cathodic reaction feasible:



Anodic Compartment

At the same time, the Cl^- anions existing in the anolyte due to the dissolution of NdCl_3 in DMSO electromigrate towards the anode and are then oxidized to gaseous $\text{Cl}_{2(g)}$ according to the following anodic reaction:



This electrolysis process was conducted galvanostatically by applying a constant current of $-30 \mu\text{A}$ at 70°C for 3 days. The results are shown in Fig. 14, where the cell, as well as cathodic potentials, are plotted against retention time.

As seen in Fig. 14b, by applying a constant current of $-30 \mu\text{A}$, the voltage initially imposed was 2.67 V, rising sharply within the first hour to 3.02 V. After this point, the cell voltage increased slowly at a rate of 6×10^{-7} V/s, reaching 3.17 V at the end of the test. Both of these observations indicate the presence of very intense non-Faradaic phenomena at the electrode–solution interface (especially at the beginning of the electrolysis test), which can be attributed to a very thick boundary layer especially at the cathode–solution interface, due to the high viscosity and therefore low conductivity of the $\text{Nd}(\text{TFSI})_3/\text{BMPTFSI}$ electrolyte, which was visible even to the naked eye (Fig. 15a, b) after the end of the electrolysis test. The

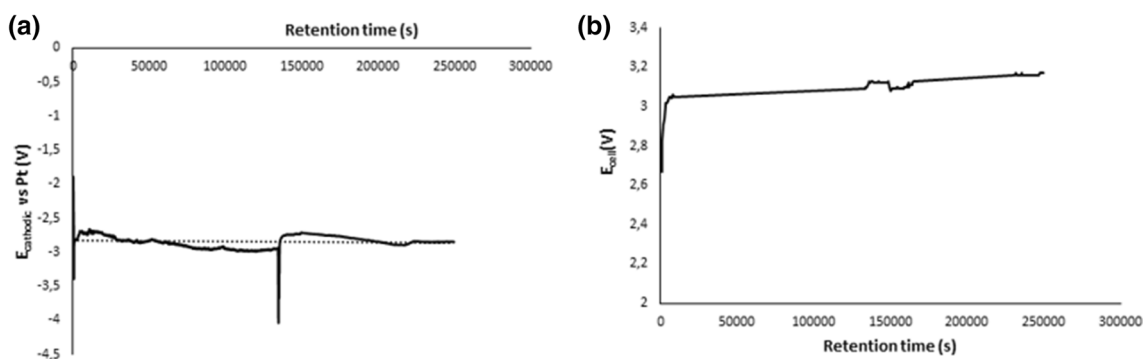


Fig. 14 **a** Cell and **b** cathodic potentials during Nd electrolysis

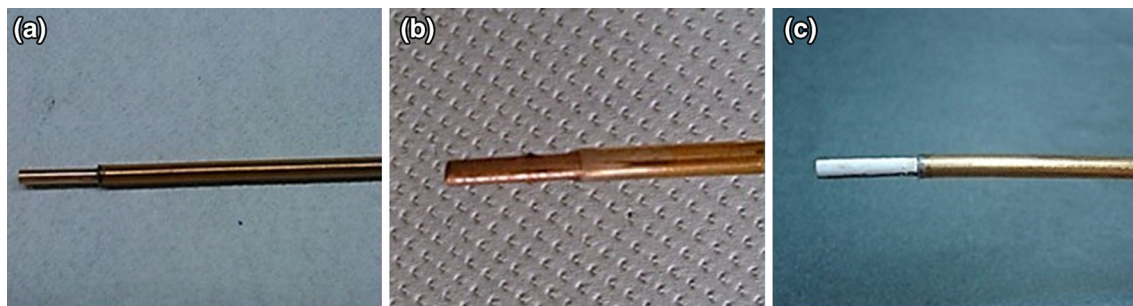


Fig. 15 **a** Cu cathode wire before the test. **b** Cu cathode after the test. **c** Cu cathode after the test and rinsing with DMSO and acetone (color figure online)

cathodic potential remained almost constant during the electrolysis with a value in the range from -2.83 to -2.85 V versus Pt (Fig. 14a).

At the end of the test, the Cu cathode was rinsed with DMSO and acetone, in order to dissolve and remove the thick layer of $\text{Nd}(\text{TFSI})_3/\text{BMPTFSI}$ electrolyte. Upon removal of the protective ionic liquid layer, the produced metallic Nd came into direct contact with atmospheric air and immediately (in a few minutes) was oxidized, forming the typical light-grayish Nd_2O_3 crystals seen in Fig. 15c. SEM images of the Cu cathode after rinsing with DMSO and acetone are shown in Fig. 16. The deposition at the cross electrode surface seems to be dense and homogeneous (Fig. 16a). A closer look at a higher magnification (Fig. 16b) reveals the presence of channels in between islands of deposited material, which is attributed to the removal of the viscous ionic liquid electrolyte from the surface of the cathode during its rinsing with DMSO and acetone. An even closer look (Fig. 16c) reveals that the islands of deposited material have a cellular structure, which is attributed again to the removal of the viscous ionic liquid electrolyte from the surface of the cathode.

EDS analysis of the deposited cellular material showed that it was composed of Nd_2O_3 , contaminated with the ionic liquid electrolyte, possibly due to incomplete rinsing

or inclusions of electrolyte within the cellular structure (Fig. 17).

To confirm the electrodeposition of metallic Nd, X-ray photoelectron spectroscopy (XPS) was performed. The electrolysis test was repeated using the same experimental conditions, but this time, after the end of electrolysis, the deposit was rinsed and stored inside a glove box under inert conditions in sealed serum bottles, to perform XPS measurements. The photoemission survey spectrum showed the presence of Nd, O, C, S, and F atoms. For this reason, Ar^+ sputtering cycles (2 kV, 1.2×10^{-6} mbar Ar) were performed in the UHV chamber; after the first sputtering cycle, no sulfur or fluorine was detected, revealing that their presence was (as supposed above) due to adsorption of the electrolyte on the surface of the deposit and not due to contamination of the deposit. The black line in the spectrum shown in Fig. 18, collected before the sputtering cycles, shows the Nd $3d$ peak of the sample; the binding energy of Nd $3d_{5/2}$ at 983.3 eV can be attributed to the Nd_2O_3 chemical state. It is obvious that sealing the samples in serum bottles after preparation as well as their introduction into the UHV chamber using a glove bag was insufficient to avoid oxidation of the surface. However, the blue line in the spectrum shown in Fig. 18, collected after several sputtering cycles, reveals a second binding energy

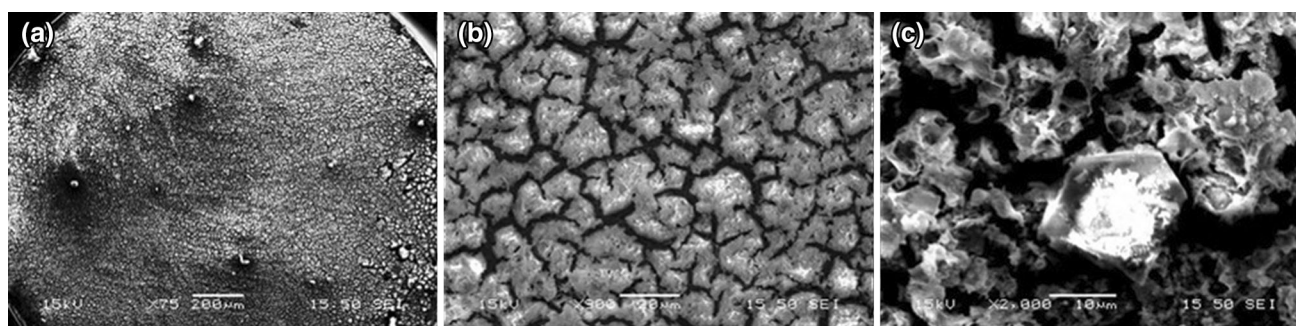
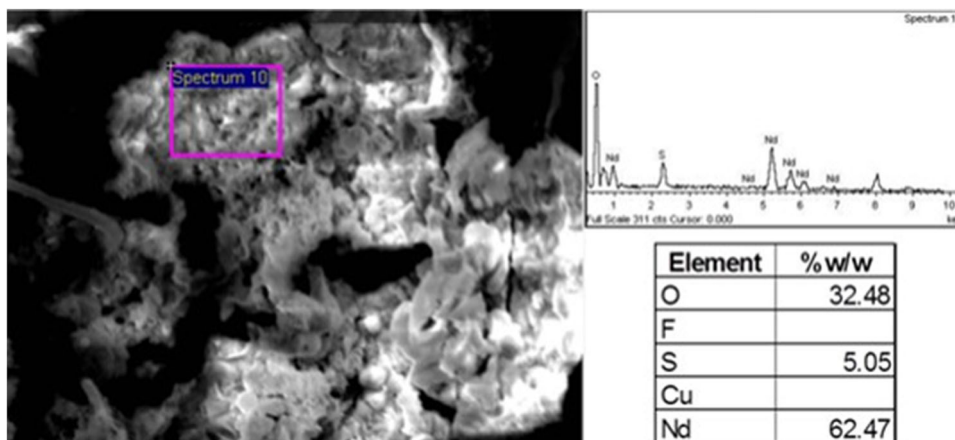


Fig. 16 SEM images of the Cu cathode after rinsing with DMSO and acetone at different magnifications: **a** $\times 75$, **b** $\times 900$, and **c** $\times 2000$

Fig. 17 Typical results of EDS analysis of the deposited cellular material (color figure online)



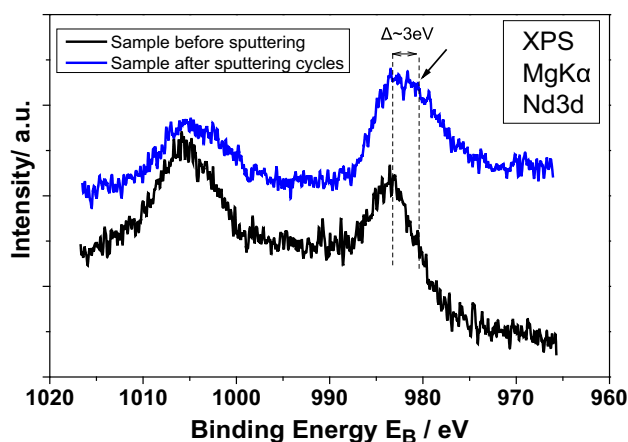


Fig. 18 XPS Nd 3d core-level spectra of the sample after introduction in UHV before (black curve) and after (blue curve) Ar⁺ sputtering (color figure online)

peak for Nd 3d_{5/2} at ~3 eV lower binding energy, which can be assigned to the Nd⁰ chemical state [27], confirming electrodeposition of metallic Nd and that any contaminants observed in the EDS spectra are due to surface adsorption of the electrolyte onto the deposit.

Conclusions

Ionic liquids are promising electrolytic media that are suitable for electrodeposition of rare-earth metals. Research in this area has proven their feasibility for reduction and electrodeposition of reactive metals, without the drawbacks presented by current technology. In this work, it was demonstrated that rare-earth metals can be successfully electrodeposited from the ionic liquids BMPTFSI and Me₃NBuTFSI at low temperature. More specifically, the electrochemical results for electrodeposition of lanthanum, neodymium, dysprosium, and samarium from BMPTFSI and lanthanum, neodymium, and samarium from Me₃NBuTFSI support these arguments, as manifested by cyclic voltammograms confirming reduction of the rare earths. Moreover, electrodeposition of the mentioned metals was successfully performed at room temperature without stirring on copper, a common substrate.

Furthermore, a two-compartment cell setup was developed and tested for electroreduction of Nd. The catholyte in the cathodic compartment was 0.05 M Nd(TFSI)₃/BMPTFSI solution, while the anolyte in the anodic compartment was 0.1 M NdCl₃/dimethylsulfoxide (DMSO) solution. The two compartments were separated through a porous semipermeable plug. Although the very small size of the electrolytic cell and the unavoidable inefficiencies (such as the high cell resistivity due to the very small

surface of the porous plug and its very high thickness-to-diameter ratio as well as the high capacitance of the electrodes due to the stationary cathode and the high electrolyte viscosity that makes the boundary layer at the electrode–solution interface very thick), the electrolytic process worked well, producing metallic Nd as confirmed by XPS analysis, indicating that the metallurgical process under development is promising.

Acknowledgements The research leading to these results has received funding from the European Community's Seventh Framework Programme (FP7/2007-2013) under Grant Agreement No. 309373. This publication reflects only the authors' views, exempting the Community from any liability. Project web site: www.eurare.eu.

References

- Ohno H (2005) *Electrochemical aspects of ionic liquids*. Wiley, New Jersey
- Tsuda T, Hussey CL (2009) *Electrochemistry of room-temperature ionic liquids and melts*. In: White RE (ed) *Modern aspects of electrochemistry*, No. 45. Springer, New York, pp 63–174
- Bockris JO, Reddy A (2002) *Modern electrochemistry: Ionics*. Kluwer Academic, New York, pp 601–654
- Ohno H (2008) *Physical properties of ionic liquids*. In: Endres F, Abbott AP, McFarlane DR (eds) *Electrodeposition from ionic liquids*, 1st edn. Wiley, Weinheim, pp 47–81
- Tsuda T, Hussey CL (2007) *Electrochemical applications of room temperature ionic liquids*. *Electrochem Soc Interface* 16:42–49
- Tian G, Li J, Hua Y (2010) *Application of ionic liquids in hydrometallurgy of nonferrous metals*. *Trans Nonferrous Met Soc China* 20:513–520
- Park J, Jung Y, Kusumah P, Lee J, Kwon K, Kyoung Lee C (2014) *Application of ionic liquids in hydrometallurgy*. *Int J Mol Sci* 15:15320–15343
- Zoski CG (2007) *Handbook of electrochemistry*. Elsevier, Amsterdam
- Cui Y, Hua Y, Lin Y (2010) *Applications of ionic liquids in electrodeposition of rare earths*. *J Chongqing Univ* 9(4):167–176
- Ispas A, Bund A (2014) *Electrodeposition from ionic liquids*. *Electrochem Soc Interface* 23:47–51
- Ispas A, Adolphi B, Bund A, Endres F (2010) *On the electrodeposition of tantalum from three different ionic liquids with the bis(trifluoromethyl sulfonyl) amide anion*. *Phys Chem Chem Phys* 12:1793–1803
- Jiang T, Chollier Brym MJ, Dubé G, Lasia A, Brisard GM (2006) *Electrodeposition of aluminium from ionic liquids: part I electrodeposition and surface morphology of aluminium from aluminium chloride (AlCl₃)–1-ethyl-3-methylimidazolium chloride ([EMIm]Cl) ionic liquids*. *Surf Coat Technol* 201:1–9
- Tsuda T, Nohira T, Ito Y (2001) *Electrodeposition of lanthanum in lanthanum chloride saturated AlCl₃-1-ethyl-3-methylimidazolium chloride molten salts*. *Electrochim Acta* 46(12):1891–1897
- Tsuda T, Nohira T, Ito Y (2002) *Nucleation and surface morphology of aluminium-lanthanum alloy electrodeposited in a LaCl₃-saturated AlCl₃-EtMeImCl room temperature molten salt*. *Electrochim Acta* 47(17):2817–2822
- Lin FM, Hussey CL (1993) *An electrochemical and spectroscopic study of cerium in the basic aluminum chloride-1-methyl-*

- ethylimidazolium chloride molten salt. *J Electrochem Soc* 140(11):3093–3096
16. Jagadeeswara RC, Venkatesan KA, Nagarajan K, Srinivasan TG, Rao PRV (2010) Electrochemical and thermodynamic properties of europium(III), samarium(III) and cerium(III) in 1-butyl-3-methylimidazolium chloride ionic liquid. *J Nucl Mater* 399(1):81–86
 17. Glukhov LM, Greish AA, Kustov LM (2010) Electrodeposition of rare earth metals Y, Gd, Yb in ionic liquids. *Russ J Phys Chem A* 84(1):104–108
 18. Legeai S, Diliberto S, Stein N, Boulanger C, Estager J, Papaiconomou N, Draye M (2008) Room-temperature ionic liquid for lanthanum electrodeposition. *Electrochem Commun* 10(11):1661–1664
 19. Yamagata M, Katayama Y, Miura T (2006) Electrochemical behavior of samarium, europium and ytterbium in hydrophobic room temperature molten salt systems. *J Electrochem Soc* 153(1):E5–E9
 20. Rao CJ, Venkatesan KA, Nagarajan K, Srinivasan TG, Rao PRV (2009) Electrochemical behavior of europium (III) in *N*-butyl-*N*-methylpyrrolidinium bis(trifluoromethylsulfonyl)imide. *Electrochim Acta* 54(20):4718–4725
 21. Hussey CL, Chou LH (2014) An electrochemical and spectroscopic study of Nd(III) and Pr(III) coordination in the 1-butyl-1-methylpyrrolidinium bis(trifluoromethylsulfonyl)imide ionic liquid containing chloride ion. *Inorg Chem* 53:5750–5758
 22. Bhatt AI, May I, Volkovich VA, Collison D, Helliwell M, Polovov IB, Lewin RG (2005) Structural characterisation of a lanthanum bistriflimide complex $\text{La}(\text{N}(\text{SO}_2\text{CF}_3)_3(\text{H}_2\text{O})_3)$ and an investigation of La, Sm and Eu electrochemistry in a room-temperature ionic liquid, $[\text{Me}_3\text{NnBu}]\text{N}(\text{SO}_2(\text{CF}_3)_2)$. *Inorg Chem* 44:4934–4940
 23. Chiappe C, Malvaldi M, Melai B, Fantini S, Bardi U, Caporali S (2009) An unusual common ion effect promotes dissolution of metal salts in room-temperature ionic liquids: a strategy to obtain ionic liquids having organic–inorganic mixed cations. *Green Chem* 12:77–80
 24. Eiden P, Liu Q, Zein El Abedin S, Endres F, Krossing I (2009) An experimental and theoretical study of the aluminium mixtures of AlCl_3 with the ionic liquids $[\text{BMP}]\text{Tf}_2\text{N}$ and $[\text{Emim}]\text{Tf}_2\text{N}$. *Chem Eur J* 15:3426–3434
 25. Rocher NM, Izgorodina EI, Rütther T, Forsyth M, McFarlane DR, Rodopoulos T, Horne MD, Bond AM (2009) Aluminium speciation in 1-butyl-1-methylpyrrolidinium bis(trifluoromethylsulfonyl)amide/ AlCl_3 mixtures. *Chem Eur J* 15:3435–3447
 26. Sasaya N, Matsumiya M, Tsunashima K (2015) Solvation and electrochemical analyses of neodymium complexes in TFSA-based ionic liquids dissolving the nitrates synthesized from spent Nd-Fe-B magnets. *Polyhedron* 85:888–893
 27. Otaa H, Matsumiya M, Sasayaa N, Nishihatab K (2016) Investigation of electrodeposition behavior for Nd(III) in $[\text{P}2225][\text{TFSA}]$ ionic liquid by EQCM methods with elevated temperatures. *Electrochim Acta* 222:20–26